

# Direct $CP$ Violation in Charmless B Decays at LHCb

*Jussara M. de Miranda, on behalf of the LHCb collaboration  
Centro Brasileiro de Pesquisas Fisicas  
Rio de Janeiro, BRAZIL*

## Abstract

Using data collected by LHCb experiment in 2011 we report the measurements of charge asymmetries in charmless decays of  $B$  mesons in two or three charged kaons or pions. We find positive charge asymmetries in the channels  $B_s^0 \rightarrow K^- \pi^+$  ( $3.3\sigma$ ),  $B^+ \rightarrow K^+ \pi^+ \pi^-$  ( $2.8\sigma$ ), and  $B^+ \rightarrow \pi^+ \pi^+ \pi^-$  ( $4.2\sigma$ ) and negative in  $B^0 \rightarrow K^+ \pi^-$  ( $6\sigma$ ),  $B^+ \rightarrow K^+ K^+ K^-$  ( $3.7\sigma$ ),  $B^+ \rightarrow K^+ K^- \pi^+$  ( $3.0\sigma$ ).

## 1 Introduction

We present recent studies from the LHCb experiment on direct  $CP$  violation in  $B$  meson charmless decays. Using data collected in 2011 we have studied the decays:  $B^0 \rightarrow K^+ \pi^-$  and  $B_s^0 \rightarrow K^- \pi^+$  [1];  $B^+ \rightarrow K^+ \pi^+ \pi^-$  and  $B^+ \rightarrow K^+ K^+ K^-$  [2] and  $B^+ \rightarrow K^+ K^- \pi^+$  and  $B^+ \rightarrow \pi^+ \pi^+ \pi^-$  [3] (complex-conjugate modes are implied except in asymmetry definitions). The main observable in all the analyses is the charge asymmetry in decay rates into a final state  $f$ , defined as  $A_{CP} = \frac{\Gamma(\overline{B} \rightarrow \overline{f}) - \Gamma(B \rightarrow f)}{\Gamma(\overline{B} \rightarrow \overline{f}) + \Gamma(B \rightarrow f)}$ . These channels have been extensively studied by the  $B$  factories and the Tevatron [4] but only now, with the large samples collected by LHCb, it was possible to establish first evidence (significance  $> 3\sigma$ ) of  $CP$  asymmetry in four of the channels. The exceptions are the well established  $B^0 \rightarrow K^+ \pi^-$  [4] for which we report on the most precise measurement and the  $B^+ \rightarrow K^+ \pi^+ \pi^-$  for which our measurement for the inclusive  $A_{CP}$  has a significance of  $2.8\sigma$ . The main features of the LHCb experiment that made this possible are: the very efficient particle identification and vertex location system, dedicated hadronic trigger and the ability to reverse the magnet polarity on the data taken [5].

$CP$  violating transitions and possible new physics effects originating in loop diagrams are accessible in all channels. The decays  $B^+ \rightarrow K^+ \pi^+ \pi^-$ ,  $B^+ \rightarrow K^+ K^+ K^-$  and  $B^0 \rightarrow K^+ \pi^-$  proceed through similar  $CP$  conserving penguin diagrams and have

access to CKM  $CP$  violating transitions  $b \rightarrow u$  at tree level. In these cases the smallness of penguin amplitudes is compensated by  $\sim \lambda^2$  factor as compared to the factor  $\sim \lambda^4$  for the tree contribution, where  $\lambda \sim 0.22$  is the expansion factor of the Wolfenstein parametrization of the CKM matrix.  $CP$  violation effects can potentially be large. The decays  $B^+ \rightarrow K^+K^-\pi^+$ ,  $B^+ \rightarrow \pi^+\pi^+\pi^-$  and  $B_s^0 \rightarrow K^-\pi^+$  access  $CP$  violating transitions  $b \rightarrow u$  and  $b \rightarrow t$  in tree and penguin diagrams respectively, both at the same order  $\sim \lambda^3$  leading to the overall penguin contribution much smaller than the tree and observation of  $CP$  violation is disfavored.

Using  $0.35 \text{ fb}^{-1}$  of  $pp$  collisions at  $\sqrt{s} = 7 \text{ TeV}$ , LHCb established the first evidence of  $CP$  violation in the  $B_s^0$  system in its decays to  $K\pi$  pairs, and also reported the most precise measurement of the  $CP$  asymmetry of  $B^0 \rightarrow K\pi$ . These results are presented in Section 2.

The three-body decays offer a good environment to study  $CP$  violation enriched by the interference pattern of the two-body resonances in the Dalitz plot. The charge asymmetry in regions of the phase space is likely to be greater than the integrated ones. With the complete data set of  $1 \text{ fb}^{-1}$  collected in 2011, we measure inclusive  $CP$  asymmetries for the three-body channels as well as their distributions in the phase space. It is a consequence of CPT invariance and unitarity that the sum of all partial decay widths of a particle should match that of its antiparticle. In fact, CPT is more restrictive. If we divide all possible decays of a particle into classes containing final states that are mutually distinct under the strong interactions, CPT imposes the particle-antiparticle match should be observed in each class [6]. Motivated by the physics, by CPT invariance that connects the decays  $K^\pm\pi^+\pi^-$  to  $K^\pm K^+K^-$  and  $K^+K^-\pi^\pm$  to  $\pi^\pm\pi^+\pi^-$  final states in two distinct classes, and also due to the experimental resemblance, it was natural to group the three-body analysis in two sets:  $B^\pm \rightarrow K^\pm\pi^+\pi^-$  and  $B^\pm \rightarrow K^\pm K^+K^-$  are described in Section 3 and  $B^\pm \rightarrow K^+K^-\pi^\pm$  and  $B^\pm \rightarrow \pi^\pm\pi^+\pi^-$  in Section 4.

## 2 Direct $CP$ violation in $B_s^0 \rightarrow K^-\pi^+$ and $B^0 \rightarrow K^+\pi^-$ decays

The probability for a  $b$  quark to decay as  $B_s^0 \rightarrow K\pi$  is about 14 times smaller than that to  $B^0 \rightarrow K\pi$ , and a stronger rejection of the combinatorial background was required. The polarity of the LHCb magnetic field is reversed from time to time in order to partially cancel the effects of instrumental charge asymmetries. Of the  $0.35 \text{ fb}^{-1}$ , about 43% was acquired with one polarity and the rest with opposite polarity. The LHCb hadronic trigger is particularly efficient for the two-body modes. It requires one very high transverse momentum good quality track in the event. To distinguish the  $K\pi$  final states we rely on the RICH particle identification system. The efficiencies and misidentification rates were carefully controlled using large calibration

data samples of  $D^* \rightarrow D\pi \rightarrow (K\pi)_D\pi$  and  $\Lambda_b \rightarrow p\pi$  decays. The raw asymmetry is computed from maximum likelihood fits to the  $K\pi$  invariant mass spectra shown in Figure 1. The raw asymmetry needs to be corrected for two residual effects. The first is induced by the detector acceptance, event reconstruction and the strong interaction of the final state particles with the detector material. The second is associated with the production of the  $B$  mesons and takes into account the dilution factor due to mixing. The overall correction to the raw asymmetry is  $\Delta A_{CP}(B^0) = -0.007 \pm 0.007$  and  $\Delta A_{CP}(B_s^0) = 0.010 \pm 0.002$ , where the errors are statistical. The final measured  $CP$  asymmetries are

$$\begin{aligned} A_{CP}(B_s^0 \rightarrow K\pi) &= 0.27 \pm 0.08(\text{stat}) \pm 0.02(\text{syst}), \\ A_{CP}(B^0 \rightarrow K\pi) &= -0.088 \pm 0.011(\text{stat}) \pm 0.008(\text{syst}), \end{aligned} \tag{1}$$

where the systematic uncertainties are dominated by the correction effects and in the case of the  $B_s^0 \rightarrow K\pi$  there is also a leading contribution from the combinatorial background description.

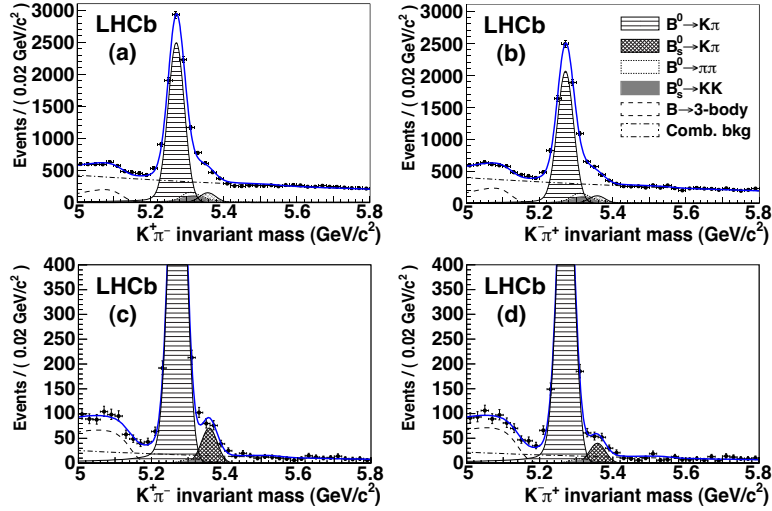


Figure 1: Invariant  $K\pi$  mass spectra obtained using the event selection adopted for best sensitivity to (a),(b) $A_{CP}(B^0 \rightarrow K\pi)$  and (c),(d) $A_{CP}(B_s^0 \rightarrow K\pi)$ . Plots (a) and (c) represent the  $K^+ \pi^-$  invariant mass whereas plots (b) and (d) represent the  $K^- \pi^+$  invariant mass. The results of unbinned maximum likelihood fits are overlaid. The main components contributing to the fit model are also shown.

### 3 Direct $CP$ violation in $B^+ \rightarrow K^+\pi^+\pi^-$ and $B^+ \rightarrow K^+K^+K^-$ decays

With relatively large branching fractions of  $\mathcal{O}(10^{-5})$  the  $B^+ \rightarrow K^+\pi^+\pi^-$  and  $B^+ \rightarrow K^+K^+K^-$  signals have comparable data samples and the analysis differs only in the particle identification and in specific peaking background estimation. The odd number of kaons in the final state and kinematics similarity enable a straight forward use of the large  $B^\pm \rightarrow J/\psi K^\pm$  control sample to account for residual effects from the production mechanism, as well as the differences in the  $K^+$  and  $K^-$  interaction with the detector material. The raw charge asymmetry,  $A_{CP}^{\text{RAW}}$ , calculated from the positive and negative event yields and the corrected  $A_{CP}$  is given by  $A_{CP}(K^\pm h^+ h^-) = A_{CP}^{\text{RAW}}(K^\pm h^+ h^-) - A_{CP}^{\text{RAW}}(J/\psi K^\pm) + A_{CP}(J/\psi K^\pm)$  where  $hh$  stands for  $KK$  or  $\pi\pi$  and the current PDG value for  $A_{CP}(J/\psi K^\pm)$  is  $(1 \pm 7) \times 10^{-3}$  [4]. The subtraction was done separately in sub samples of the data divided by trigger selections, in order to cancel a possible trigger asymmetry for kaons. The total event yields are listed in Table 1 determined from unbinned extended maximum likelihood fits to the  $B^\pm$  candidate invariant masses in the range  $5079 - 5479 \text{ MeV}/c^2$ .

The final results for the inclusive charge asymmetries of  $B^\pm \rightarrow K^\pm\pi^+\pi^-$  and  $B^\pm \rightarrow K^\pm K^+ K^-$  are:

$$A_{CP}(B^\pm \rightarrow K^\pm\pi^+\pi^-) = +0.034 \pm 0.009(\text{stat}) \pm 0.004(\text{syst}) \pm 0.007(J/\psi K^\pm),$$

$$A_{CP}(B^\pm \rightarrow K^\pm K^+ K^-) = -0.046 \pm 0.009(\text{stat}) \pm 0.005(\text{syst}) \pm 0.007(J/\psi K^\pm),$$

where the first uncertainty is statistical, the second is systematic, and the third is the uncertainty of the  $A_{CP}$  of  $B^\pm \rightarrow J/\psi K^\pm$  from the PDG [4]. The main contributions to the systematic uncertainty are attributed to the use of the control channel to account for residual asymmetries to signal model and to the acceptance in the Dalitz plot.

The two relevant variables used to represent the Dalitz plot are the two-body invariant masses ( $m_{\pi^+\pi^-}^2, m_{K^\pm\pi^\mp}^2$ ) in the case of  $B^\pm \rightarrow K^\pm\pi^+\pi^-$  decay and ( $m_{K^+K^-}^2_{\text{low}}, m_{K^+K^-}^2_{\text{high}}$ ) in the case of  $B^\pm \rightarrow K^\pm K^+ K^-$  decay, where the symmetrical phase space is folded. To visualise the asymmetries in phase space, the Dalitz plots of candidates with three-body invariant masses within  $\pm 40 \text{ MeV}/c^2$  of the peak were divided into bins with equal population using an adaptive binning algorithm. In each bin, the variable  $A_{CP}^N \equiv \frac{N^- - N^+}{N^- + N^+}$  was computed from the number of  $B^\pm$  event candidates,  $N^\pm$ ,

mode	$K^\pm\pi^+\pi^-$	$K^\pm K^+ K^-$	$J/\psi K^\pm$	$\pi^\pm\pi^+\pi^-$	$K^+K^-\pi^\pm$
$B^-$	$18\,168 \pm 170$	$10\,289 \pm 110$	$30\,140 \pm 179$	$2718 \pm 71$	$619 \pm 47$
$B^+$	$17\,540 \pm 169$	$11\,606 \pm 117$	$30\,984 \pm 182$	$2111 \pm 66$	$875 \pm 50$

Table 1: Event yields for  $B^-$  and  $B^+$  samples and for the whole data set.

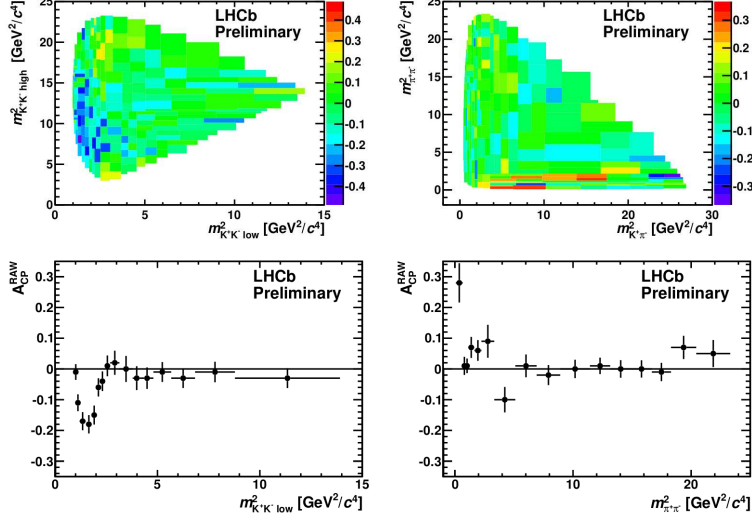


Figure 2:  $A_{CP}^N$  in Dalitz plot bins with equal event populations for  $B^\pm \rightarrow K^\pm K^+ K^-$  (top left) and  $B^\pm \rightarrow K^\pm \pi^+ \pi^-$  (top right). The asymmetry  $A_{CP}^N$  is calculated from the bin contents including backgrounds, and is not corrected for production or detection asymmetries.  $A_{CP}^{\text{RAW}}$  for  $m_{K^+K^-}^2$  (bottom left) and  $m_{\pi^+\pi^-}^2$  (bottom right) projections.

which includes signal and background events in that bin and is not corrected for efficiency. The resulting  $A_{CP}^N$  distributions over the Dalitz plots are shown in the upper plots of Figure 2. Large asymmetries are clearly visible in the low  $m_{K^+K^-}^2$  and low  $m_{\pi^+\pi^-}^2$  regions respectively for  $B^\pm \rightarrow K^\pm K^+ K^-$  and  $B^\pm \rightarrow K^\pm \pi^+ \pi^-$ .

To analyse the  $CP$  asymmetries over the phase space without background influence, the raw asymmetries were plotted in bins of the two-body invariant mass projections, shown in the bottom plots of Figure 2. We observe large opposite sign asymmetries in the low  $m_{\pi^+\pi^-}^2$  and  $m_{K^+K^-}^2$  invariant masses not clearly associated to a resonant state.

## 4 Direct $CP$ violation in $B^+ \rightarrow K^+ K^- \pi^+$ and $B^+ \rightarrow \pi^+ \pi^+ \pi^-$ decays

The samples of  $B^+ \rightarrow K^+ K^- \pi^+$  and  $B^+ \rightarrow \pi^+ \pi^+ \pi^-$  are of comparable sizes, much smaller than the  $B^+ \rightarrow K^+ \pi^+ \pi^-$  and  $B^+ \rightarrow K^+ K^+ K^-$  ones and with much higher background levels. We measure the raw asymmetry defined in terms of the  $B^+$  and  $B^-$  event yields and corrected by the acceptance in the Dalitz plot as  $^{\text{ACC}}A_{CP}^{\text{RAW}} = \frac{(N_{B^-}/R) - N_{B^+}}{(N_{B^-}/R) + N_{B^+}}$ , where  $R$  is the ratio between the  $B^+$  and  $B^-$  data-weighted average efficiency in the Dalitz plot, found to be  $R_{\pi\pi\pi} = 1.023 \pm 0.029$  and  $R_{KK\pi} = 0.991 \pm$

0.027. The total signal yields are listed in Table 1.

Here the net strangeness in the final state is zero and the residual detection asymmetry refers to a pion and is measured by LHCb to be  $A_{\text{D}}^{\pi} = (0.00 \pm 0.25)\%$  [7] using large  $D^{*\pm}$  calibration samples. The residual production asymmetry is estimated from the  $B^{\pm} \rightarrow J/\psi K^{\pm}$  control channel, eliminating the factor relative to the detection associated to bachelor kaon measured from calibration samples, to be  $A_{\text{D}}^K = -0.010 \pm 0.002$  [1].

In order to cancel out a possible trigger asymmetry for hadrons, the final asymmetries are calculated from data divided into two subsamples depending on the trigger selection. The inclusive  $CP$  asymmetries are the weighted averages of the trigger subsamples and are measured to be

$$\begin{aligned} A_{CP}(B^{\pm} \rightarrow \pi^{\pm}\pi^{+}\pi^{-}) &= +0.120 \pm 0.020(\text{stat}) \pm 0.019(\text{syst}) \pm 0.007(J/\psi K^{\pm}), \\ A_{CP}(B^{\pm} \rightarrow K^{+}K^{-}\pi^{\pm}) &= -0.153 \pm 0.046(\text{stat}) \pm 0.019(\text{syst}) \pm 0.007(J/\psi K^{\pm}), \end{aligned}$$

where the first uncertainty is statistical, the second is the experimental systematic uncertainty, and the third is the uncertainty of the  $A_{CP}$  value of  $B^{\pm} \rightarrow J/\psi K^{\pm}$  from the PDG [4].

Investigating the distribution of asymmetries in the Dalitz plots we observe large negative contributions at low  $m_{K^{+}K^{-}}^2$  invariant mass as well as large positive asymmetries at low  $m_{\pi^{+}\pi^{-}}^2$ , particularly in the high  $m_{\pi^{+}\pi^{-}}^2$  region, as can be seen in Figures 3 and 4. To quantify this effect we compute the local  $CP$  asymmetry in the phase space regions in the same way as the inclusive one, correcting for the acceptance, production asymmetry and detection asymmetry. The  $CP$  asymmetry of  $B^{\pm} \rightarrow \pi^{\pm}\pi^{+}\pi^{-}$  in the region  $m_{\pi^{+}\pi^{-}}^2$  low  $< 0.4 \text{ GeV}^2/c^4$  and  $m_{\pi^{+}\pi^{-}}^2$  high  $> 15 \text{ GeV}^2/c^4$  is determined to be

$$A_{CP}(B^{\pm} \rightarrow \pi^{\pm}\pi^{+}\pi^{-} \text{ region}) = +0.622 \pm 0.075(\text{stat}) \pm 0.032(\text{syst}) \pm 0.007(J/\psi K^{\pm}).$$

The  $CP$  asymmetry of  $B^{\pm} \rightarrow K^{+}K^{-}\pi^{\pm}$  in the region  $m_{K^{+}K^{-}}^2 < 1.5 \text{ GeV}^2/c^4$  is measured to be

$$A_{CP}(B^{\pm} \rightarrow K^{+}K^{-}\pi^{\pm} \text{ region}) = -0.671 \pm 0.067(\text{stat}) \pm 0.028(\text{syst}) \pm 0.007(J/\psi K^{\pm}).$$

## 5 Conclusion

We have observed a rich pattern of  $CP$  violation in the charmless decays of the  $B$  mesons. Contrary to naive expectations, we observe large  $CP$  violation in the  $B^{+} \rightarrow K^{+}K^{-}\pi^{+}$ ,  $B^{+} \rightarrow \pi^{+}\pi^{+}\pi^{-}$ . Intriguingly large opposite sign  $A_{CP}$  is observed in the low  $K^{+}K^{-}$  and  $\pi^{+}\pi^{-}$  invariant mass regions of the three-body decays. The effect seems not to be associated to any resonant state. LHCb will triple its sample with the data collected in 2012.

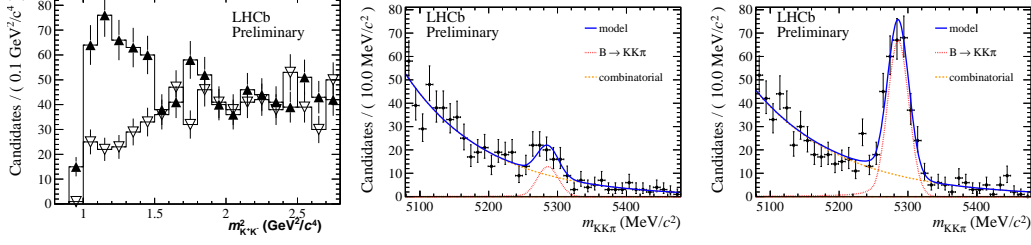


Figure 3:  $B^\pm \rightarrow K^+K^-\pi^\pm$  event yields (signal and background) as a function of  $m_{K^+K^-}^2$  (left), where the empty triangles represent  $B^-$  and the filled triangles represent  $B^+$ ; fits of  $B^-$  (center) and  $B^+$  (right) for candidates with  $m_{K^+K^-}^2 < 1.5 \text{ GeV}^2/c^4$ .

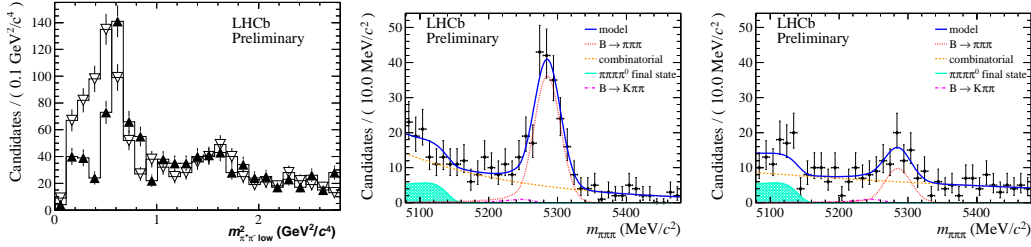


Figure 4:  $B^\pm \rightarrow \pi^\pm\pi^+\pi^-$  event yields (signal and background) as a function of  $m_{\pi^+\pi^-\text{low}}^2$  for  $m_{\pi^+\pi^-\text{high}}^2 > 15 \text{ GeV}^2/c^4$  (left), where the empty triangles represent  $B^-$  and the filled triangles represent  $B^+$ ; and fits of  $B^-$  (center) and  $B^+$  (right) for candidates with  $m_{\pi^+\pi^-\text{low}}^2 < 0.4 \text{ GeV}^2/c^4$  and  $m_{\pi^+\pi^-\text{high}}^2 > 15 \text{ GeV}^2/c^4$ .

## References

- [1] R. Aaij *et al.* [LHCb Collaboration], Phys. Rev. Lett. **108**, 201601 (2012) [arXiv:1202.6251 [hep-ex]].
- [2] R. Aaij *et al.* [LHCb Collaboration], LHCb-CONF-2012-018
- [3] R. Aaij *et al.* [LHCb Collaboration], LHCb-CONF-2012-028
- [4] K. Nakamura *et al.* [Particle Data Group Collaboration], J. Phys. G **37**, 075021 (2010).
- [5] A. A. Alves, Jr. *et al.* [LHCb Collaboration], JINST **3**, S08005 (2008).
- [6] I. I. Y. Bigi and A. I. Sanda, Camb. Monogr. Part. Phys. Nucl. Phys. Cosmol. **28**, 1 (2009).

- [7] RAaij *et al.* [LHCb Collaboration], Phys. Lett. B **713**, 186 (2012)  
[arXiv:1205.0897 [hep-ex]].